Endothelial barrier stabilization by a cyclic tandem peptide targeting VE-cadherin transinteraction in vitro and in vivo

Wolfgang-Moritz Heupel[1,*], Athina Efthymiadis[1,*], Nicolas Schlegel[1], Thomas Müller[2], Yvonne Baumer[1], Werner Baumgartner[3], Detlev Drenckhahn[1,‡] and Jens Waschke[1,‡]

[1]University of Würzburg, Institute of Anatomy and Cell Biology, Koellikerstr. 6, D-97070 Würzburg, Germany
[2]University of Würzburg, Department of Botany I, Julius-von-Sachs-Platz 2, D-97082 Würzburg, Germany
[3]RWTH Aachen, Institute of Biology II, Kopernikusstr. 16, D-52056 Aachen, Germany

*These authors contributed equally to this work
‡Authors for correspondence: (e-mails: jens.waschke@mail.uni-wuerzburg.de; drenckhahn@uni-wuerzburg.de)

Accepted 28 January 2009
Journal of Cell Science 122, 1616-1625 Published by The Company of Biologists 2009
doi:10.1242/jcs.040212

Summary

Inflammatory stimuli result in vascular leakage with potentially life threatening consequences. As a key barrier component, loss of vascular endothelial (VE-) cadherin-mediated adhesion often precedes endothelial breakdown. This study aimed to stabilize VE-cadherin transinteraction and endothelial barrier function using peptides targeting the VE-cadherin adhesive interface. After modelling the transinteracting VE-cadherin structure, an inhibiting single peptide (SP) against a VE-cadherin binding pocket was selected, which specifically blocked VE-cadherin transinteraction as analyzed by single molecule atomic force microscopy (AFM). The tandem peptide (TP) consisting of two SP sequences in tandem was designed to strengthen VE-cadherin adhesion by simultaneously binding and cross-bridging two interacting cadherin molecules. Indeed, in AFM experiments TP specifically rendered VE-cadherin transinteraction resistant against an inhibitory monoclonal antibody. Moreover, TP reduced VE-cadherin lateral mobility and enhanced binding of VE-cadherin-coated microbeads to cultured endothelial cells, but acted independently of the actin cytoskeleton. TP also stabilized endothelial barrier properties against the Ca^{2+} ionophore A23187 and the inhibitory antibody. Finally, TP abolished endothelial permeability increase induced by tumour necrosis factor-α in microperfused venules in vivo. Stabilization of VE-cadherin adhesion by cross-bridging peptides may therefore be a novel therapeutic approach for the treatment of vascular hyperpermeability.

Key words: VE-cadherin, Endothelial barrier, TNF-α, Peptide, Inflammation

Introduction

Cadherins are essential for cell adhesion and critically involved in various physiological and pathological processes (Angst et al., 2001; Gumbiner, 2000). The cadherin superfamily comprises Ca^{2+}-dependent single-span transmembrane glycoproteins interacting with cadherins of neighbouring cells in homophilic and heterophilic fashion to confer cell adhesion and recognition (Angst et al., 2001; Steinberg and McNutt, 1999; Yap et al., 1997). Crystal structures for C- and N-cadherin revealed a pair of molecules interacting as a symmetric dimer formed through the interaction of the partner extracellular EC1 domains (Boggon et al., 2002; Shapiro et al., 1995). The cytoplasmic domain is responsible for the linkage of cadherins to the actin cytoskeleton via catenins, thereby providing strength and cohesion to adherence junctions (Baumgartner et al., 2003; Navarro et al., 1995).

Vascular endothelial (VE-) cadherin is the predominant cadherin expressed in endothelial cells and has been shown to be essential for stabilizing the endothelial lining of the inner surface of blood vessels and for regulating the barrier between blood and surrounding tissues (Dejana et al., 2008; Vandenbroucke et al., 2008). Loss of VE-cadherin function in pathological processes has been demonstrated (Alexander and Elrod, 2002; Corada et al., 1999; Hordijk et al., 1999) and VE-cadherin was found to be one of the target molecules modulated by signalling of several inflammatory mediators such as histamine, thrombin and tumour necrosis factor-α (TNF-α) (Andriopoulou et al., 1999; Angelini et al., 2006; Konstantoulaki et al., 2003; Nwariaku et al., 2002; Rabiet et al., 1994; Rabiet et al., 1996). The impact of loss of VE-cadherin function was further demonstrated in vivo where vascular permeability was increased after application of the VE-cadherin-specific monoclonal antibody (mAb) 11D4.1 (Corada et al., 1999). Specific stabilization of VE-cadherin binding could therefore be a promising way to prevent endothelial barrier breakdown. For N-cadherin, it was demonstrated that application of peptides consisting of dimeric N-cadherin binding motifs promoted neurite outgrowth and were therefore considered N-cadherin agonists (Williams et al., 2002). A similar approach that might also be promising would be to modulate VE-cadherin-mediated adhesion: by tandem peptide-mediated cross-bridging of VE-cadherin molecules we sought to strengthen VE-cadherin adhesion and thereby protect endothelial barrier function under conditions where VE-cadherin transinteraction is compromised.

To address this, we modelled the protein sequence of VE-cadherin into the resolved structure of E-cadherin (Nagar et al., 1996) and shaped the transinteracting VE-cadherin surface of the two outermost extracellular domains. By this approach, a single peptide (SP) sequence was selected which fitted into the probable binding interface of VE-cadherin. This peptide was expected to inhibit VE-cadherin transinteraction. A tandem peptide (TP) was then generated by connecting two consecutive SP sequences with a flexible linker. TP was supposed to stabilize VE-cadherin transinteraction by

simultaneously binding to the adhesive interfaces of two interacting VE-cadherin molecules. The proof of function of these peptides was tested by single molecule atomic force microscopy (AFM), fluorescent recovery after photobleaching (FRAP), laser tweezers and measurements of transendothelial resistance (TER). Finally, permeability measurements in individually perfused rat mesenteric venules demonstrated that TP also prevented TNF-α-induced breakdown of endothelial barrier function in vivo.

Results

Model structure of the VE-cadherin-specific peptides

A homology-based model for transinteracting VE-cadherin molecule pairs (Fig. 1A) suggested a small segment of the sequence derived from β4-strand (residues Arg47 to Glu51; Fig. 1B,C) of the N-terminal VE-cadherin domain 1 as a possible inhibitor because of its involvement in general VE-cadherin transinteraction. This segment exhibited high sequence homology with mouse and rat VE-cadherin. In our interaction model Arg47 of this RVDAE sequence tightly interacts via hydrogen bonds with the sidechain and mainchain groups of the peptide stretch Thr80 to Glu82 of VE-cadherin (Fig. 1D). Asp49 also forms a putative H-bond with the mainchain amide of Thr80, and the amide group of Ala50 is hydrogen-bonded to the backbone carbonyl group of Asp79. Glu51 can possibly form two salt-bridge interactions with the side-chain amino groups of Lys34 and Lys78. Thus, this short pentapeptide should bind with reasonable affinity to residues in the β6β7-sheet of the complementary transinteracting VE-cadherin molecule. Molecular simulations using the peptide-VE-cadherin complex confirmed a stable interaction between the two molecules, consistent with the experimental interaction studies (see below). Fig. 1E depicts a model of the tandem peptide, which is cyclized via two cysteine residues at the N- and C-terminus and a 6-aminohexanoic acid linker.

Characterization of SP and TP action in cell-free AFM experiments: SP blocked homophilic VE-cadherin transinteraction whereas TP prevented the effects of an inhibitory VE-cadherin antibody

As a proof of principle, we first studied the effect of the designed peptides in cell-free AFM experiments (Fig. 2). Recombinant VE-cadherin molecules were covalently coupled to tip and plate of the AFM setup to probe homophilic VE-cadherin transinteraction via force distance cycles. In order to find optimal peptide concentrations, dose-response experiments investigating the effect of SP and TP on VE-cadherin transinteraction were performed (Fig. 2A). VE-cadherin binding was evaluated via quantification of binding activities revealing the amount and extend of VE-cadherin transinteraction as a combination of single molecule binding probabilities, unbinding forces and multi-bond ruptures (see Materials and Methods section). SP significantly reduced VE-cadherin binding activity at concentrations starting from 20 μM. At a concentration of 200 μM, binding activity was reduced to about 30% of control levels, whereas higher doses had no additional effect. Similar reductions were also observed in Ca^{2+}-free conditions demonstrating Ca^{2+}-dependent binding of VE-cadherin. To achieve maximal inhibitory effects, SP was therefore used at a concentration of 200 μM in further experiments. In clear contrast, a right-shifted dose-response curve was obtained in TP experiments. TP led to decreased binding activity only at higher concentrations compared with SP. Inhibitory action at high concentrations of TP was expected because saturation of all VE-cadherin binding sites by TP would prevent cross-bridging of adjacent VE-cadherin molecules and thus would result in decreased binding activity. However, significantly increased VE-cadherin binding activity was not observed at any TP concentration investigated. Therefore, to avoid possible inhibitory effects, TP was used at 20 μM in all further experiments.

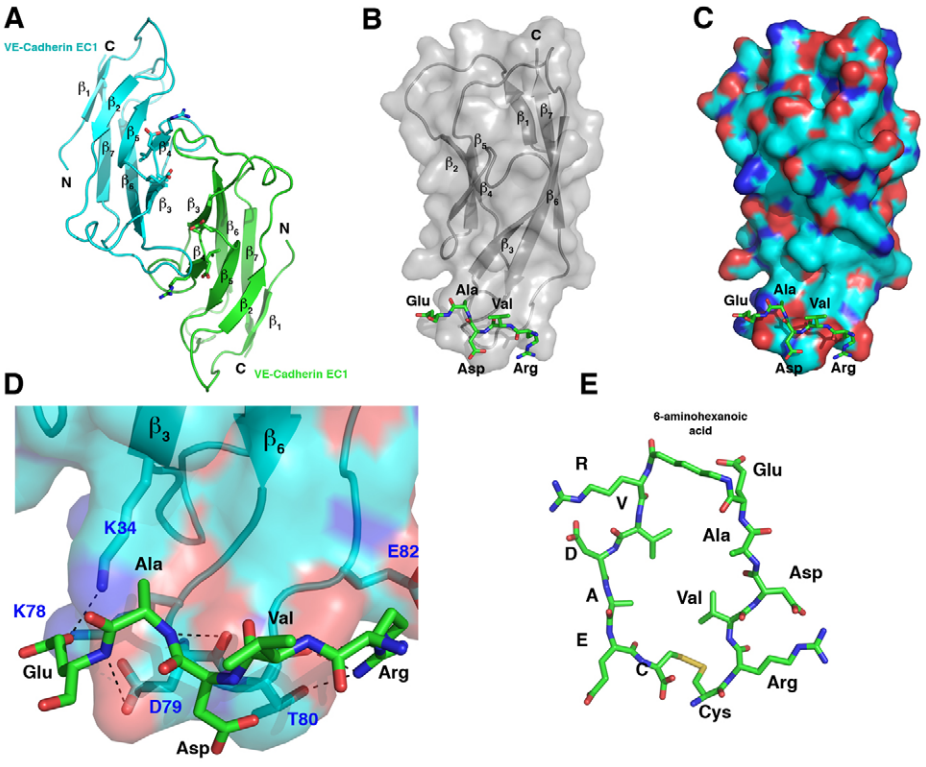

Fig. 1. Structure of VE-cadherin, and peptide design. (A) Model of a *trans*-interacting VE-cadherin EC1 pair. Secondary structure elements and N- and C-termini are indicated. Side chains of the RVDAE motif are shown in stick format. (B) Docking of the RVDAE peptide onto the surface of a VE-cadherin EC1 module (grey with transparent surface). (C) Same as in B but with the surface of VE-cadherin EC1 colour-coded according to polarity: blue, nitrogen atoms; cyan, carbon atoms; red, oxygen atoms. (D) Magnification of the peptide binding site. Putative hydrogen bonds between the peptide and the EC1 domain of VE-cadherin are shown as dashed lines. (E) Model of the tandem peptide, which is cyclized by two cysteine residues at the N- and C-terminus and a 6-aminohexanoic acid linker.

Next, VE-cadherin unbinding forces under different peptide conditions were analyzed in force-distance cycles in detail (for representative cycles see Fig. 2B). As shown in Fig. 2C, under control conditions three distinct unbinding force peaks were observed in frequency distribution analyses of >500 unbinding curves at retrace velocities of 600 nm/second (f_1=35 pN; f_2=62 pN; f_3=108 pN). This is consistent with our previous observations and has been explained by lateral oligomerization and cooperative unbinding of cadherin dimers (Baumgartner et al., 2000). The first unbinding peak was further in the range of rupture forces determined for VE-cadherin molecules of opposing cells (Panorchan et al., 2006). When TP was applied at 20 μM, a shift towards the first unbinding force peak was observed (61% versus 50% of total unbinding events, respectively; see insets in Fig. 2C which show Gaussian multiple peak fittings of probability density curves for control and TP condition). By contrast, in the presence of SP (200 μM) VE-cadherin transinteraction revealed distinct but strongly reduced force peaks because probability density curves were corrected by normalization with evaluated interaction frequencies (single molecule interaction frequencies were 52.8%, 54.0% and 20.3% in control, TP and SP condition, respectively). These experiments indicate that TP stabilized VE-cadherin dimers involving two VE-cadherin-Fc molecules but did not result in altered single molecule unbinding forces themselves. Increasing retrace velocities led to a logarithmic increase in unbinding forces as expected but revealed comparable effects of peptides on VE-cadherin unbinding forces (data not shown).

Having characterized peptide effects on VE-cadherin transinteraction, specificity and protective effects were evaluated. Fig.

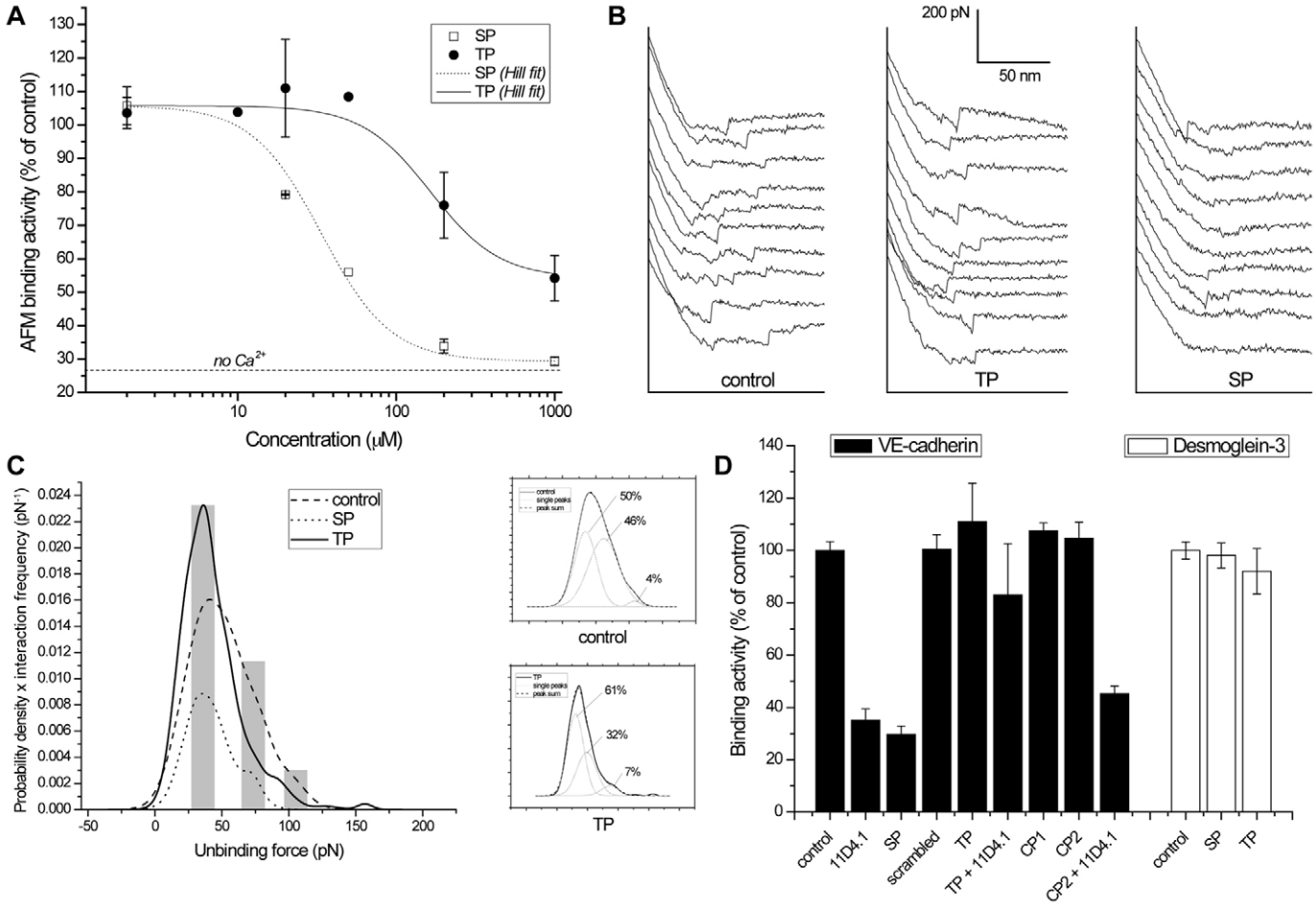

Fig. 2. Effect of SP and TP on single molecule VE-cadherin transinteraction. (A) Dose-response curves show action of SP and TP on VE-cadherin transinteraction as probed by AFM single molecule unbinding studies. SP reduced VE-cadherin binding activity at concentrations of 20 μM or higher, resulting in a reduction of about 70% at 200 μM. By contrast, TP displayed a shifted dose-response curve with inhibiting activity starting at 200 μM. The dashed line indicates VE-cadherin binding activity in Ca^{2+}-free conditions. (B) Sample force-distance cycles in control, 20 μM TP or 200 μM SP conditions. Note the similar unbinding events in TP and control conditions but reduced interaction frequency in SP condition. (C) Frequency distribution of single molecule VE-cadherin-Fc unbinding events measured at retrace velocities of 600 nm/second. For each condition, >500 unbinding curves were evaluated and resulting probability densities corrected by interaction frequencies, which were 52.8% for control, 54.0% for TP and 20.3% for SP condition. In control conditions, three different force peaks could be differentiated (marked by grey columns). Note the frequency increase for the first unbinding force peak in TP condition (61% versus 50%; see also insets with Gaussian multiple peak fits of control and TP probability density curves) and reduced interaction frequency after SP treatment. (D) Binding activities of transinteracting VE-cadherin-Fc were strongly reduced after treatment with monoclonal VE-cadherin antibody 11D4.1. As already demonstrated in A, SP at 200 μM blocked VE-cadherin transinteraction whereas TP at 20 μM did not. Preincubation with 20 μM TP, however, prevented 11D4.1-induced loss of VE-cadherin adhesion. Sequence specificity of SP and TP action was demonstrated by a scrambled SP or control peptides CP1 and CP2, which did not have an effect on VE-cadherin binding activity, and by CP2 which was unable to block 11D4.1-mediated inhibition. Moreover, SP and TP at the concentrations used did not influence transinteraction of desmonglein-3-Fc (n=3–4 for each condition).

2D summarizes AFM data of VE-cadherin binding activities under conditions using control peptides or TP in the presence or absence of mAb 11D4.1. Treatment with 11D4.1 resulted in significantly reduced binding activity (35±4% of controls), indicating specificity of VE-cadherin interactions in the AFM setup. SP (200 μM) was found to efficiently reduce VE-cadherin transinteraction to 30±3% of control levels, whereas TP (20 μM) did not significantly alter VE-cadherin binding activities. Next, we investigated whether TP was effective in preventing loss of VE-cadherin binding induced by mAb 11D4.1 because we assumed that TP would stabilize VE-cadherin transinteraction. Interestingly, preincubation with TP blocked mAb 11D4.1-induced loss of transinteraction (binding activities were 83±20% of controls). Sequence specificity of SP and TP action was further demonstrated by a scrambled SP or control peptides CP1 and CP2. CP1 is a SP peptide specific for desmoglein transinteraction and CP2 the tandem version of CP1 (Heupel et al., 2009). All three control peptides did not affect VE-cadherin binding activity, and dimeric CP2 was not effective at blocking mAb 11D4.1-mediated inhibition of VE-cadherin transinteraction. In a parallel set of experiments, SP and TP were shown not to interfere with transinteraction of a member of the desmocadherin family, desmoglein-3-Fc, indicating that the effect on VE-cadherin transinteraction was not due to unspecific effects of the peptides. Taken together, AFM experiments demonstrated that SP efficiently inhibited homophilic VE-cadherin transinteraction demonstrating SP binding to the proposed binding pocket. TP, however, enhanced VE-cadherin-Fc dimer interactions and effectively inhibited antibody-induced loss of VE-cadherin binding.

SP and TP peptides modified lateral diffusion of VE-cadherin-EYFP

To directly investigate effects of SP and TP on VE-cadherin lateral mobility, we used FRAP studies in a cell line stably expressing VE-cadherin-EYFP (CHO-A1; Fig. 3A). In CHO-A1 cells, VE-cadherin-EYFP signals were confined to sites of cell-cell contacts. EYFP signals were specifically bleached at regions of cell-cell contacts and subsequent increases in fluorescence signals were measured over time. In controls, VE-cadherin-EYFP displayed a biphasic, double-exponential recovery after photobleaching with a rapid recovery of the signal within a few seconds followed by a steady increase afterwards (Fig. 3B). Also, a rather slow recovery and high fraction of immobile molecules was noted under all conditions tested, as typically seen for other adhesion molecules (Stehbens et al., 2006). Compared with controls, SP led to a significant increase in fluorescence recovery indicating enhanced lateral diffusion of VE-cadherin-EYFP, probably because of SP-induced interference with VE-cadherin interactions (see Fig. 2D). By contrast, TP treatment resulted in decreased signal recovery. This suggested diminished lateral diffusion of VE-cadherin in response to TP-induced stabilization of VE-cadherin interactions.

TP prevented reduction of VE-cadherin bead binding induced by mAb 11D4.1 and the Ca^{2+} ionophore A23187 but acted independently of cytoskeletal anchorage or signalling

We further investigated whether TP treatment had a protective effect on endogenous VE-cadherin binding using laser tweezer experiments with VE-cadherin-coated microbeads (Fig. 4A). Beads were seeded on the surface of endothelial MyEnd cells to allow formation of cell-to-bead contacts as characterized in detail previously (Baumgartner et al., 2003). After 30 minutes, beads were exposed to a laser beam to test bead binding. The number of beads

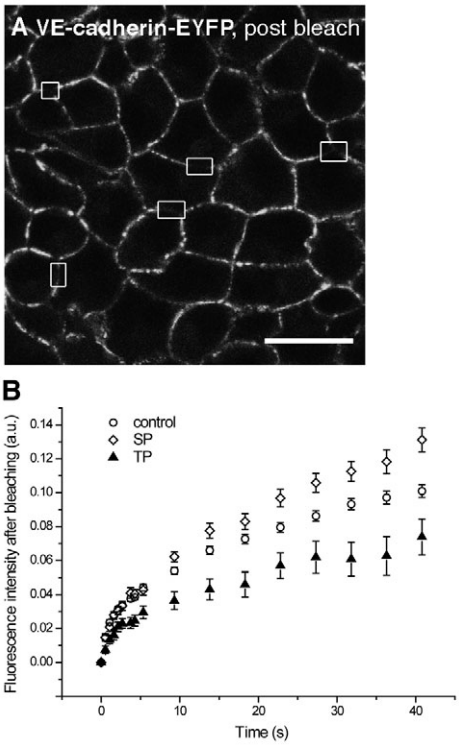

Fig. 3. SP and TP peptides modified lateral diffusion of VE-cadherin-EYFP in FRAP studies. (A) In CHO-A1 cells, VE-cadherin-EYFP signals were continuously seen at sites of cell-cell contacts. In this sample post-bleach image, rectangles indicate region of interests where EYFP fluorescence had just been bleached at sites of cell-cell contacts. Scale bar: 20 μm. (B) Measurements of fluorescence intensities in these regions showed a biphasic, double-exponential recovery of EYFP signals after bleaching in all three conditions. After $t \approx 9$ seconds, however, VE-cadherin-EYFP recovery was enhanced in SP-pretreated cells, whereas it was reduced during nearly the whole time series in TP-pretreated cells. Note the overall slow recovery and high fraction of immobile molecules in all conditions.

resisting displacement by the laser beam was counted after 30 minutes (69±3%), taken as tightly bound and set to 100% (Fig. 4B). Preincubation with TP for 30 minutes before bead binding led to a significant increase of bound beads in MyEnd cells (115±2%). Incubation of bound beads with mAb 11D4.1 resulted in a strong reduction of VE-cadherin-mediated bead binding (63±2%). This antibody-mediated weakening of binding was completely prevented by preincubation of MyEnd cells with TP (10±3%). Similar experiments were performed using the Ca^{2+} ionophore A23187, which had been shown to result in dissociation of cell-cell junctions and increased permeability in vivo and in vitro, at least in part by targeting VE-cadherin cytoskeletal anchorage (Baumgartner et al., 2003; Curry et al., 1990; He and Curry, 1991; Schnittler et al., 1990). A23187 treatment for 45 minutes strongly reduced the number of bound beads (68±4%). However, in the presence of TP, A23187-induced loss of bead binding was completely prevented (97±2%).

We have shown previously that immobilization of VE-cadherin molecules by linkage to the actin cytoskeleton significantly improved VE-cadherin-mediated bead binding (Baumgartner et al., 2003). Addition of the F-actin-disrupting agent cytochalasin D (10 μM) for 30 minutes to endothelial monolayers with surface-bound beads strongly reduced bead binding to 55±4% of controls (Fig. 4B). Importantly, TP largely prevented cytochalasin D-induced

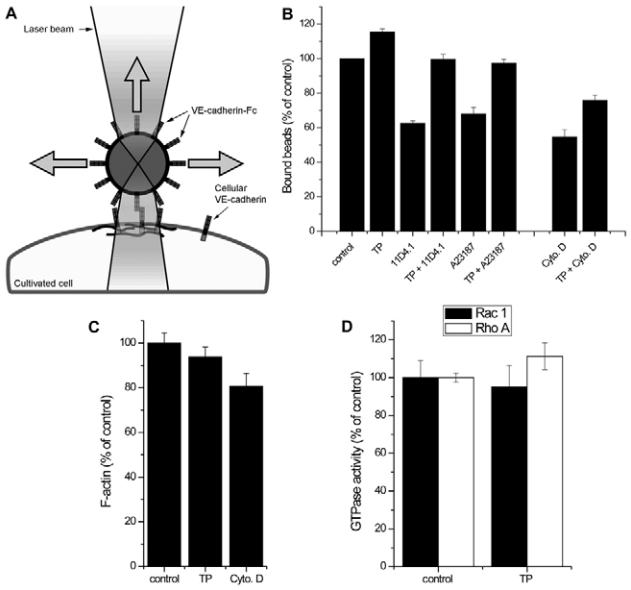

Fig. 4. TP prevented mAb 11D4.1- and A23187-induced loss of VE-cadherin-mediated adhesion but acted independently of F-actin or Rho GTPase function. (A) Principle of laser tweezer experiments. VE-cadherin-coated microbeads were allowed to settle on the surface of MyEnd cells to induce VE-cadherin-mediated homophilic adhesion. Afterwards, beads were trapped in a laser beam focus to discriminate bound from unbound beads. (B) On MyEnd cells, the number of bound beads was significantly increased after incubation with TP for 30 minutes, compared with controls. Incubation with mAb 11D4.1 led to a strong loss of VE-cadherin bead binding. Preincubation with TP (20 μM), however, completely prevented this reduction. Incubation with the Ca^{2+} ionophore A23187 (10 μM) for 45 minutes similarly reduced bead binding, whereas preincubation with TP (20 μM) again completely blocked this effect. Incubation with the F-actin-disrupting agent cytochalasin D (10 μM) for 30 minutes strongly reduced the number of surface-bound beads. Nevertheless, preincubation with TP in combination with cytochalasin D resulted in increased bead binding compared to cytochalasin D alone (n=6–8). (C) Quantification of F-actin demonstrated that only cytochalasin D but not TP treatment significantly decreased the F-actin content. (D) In GTPase activity assays, TP treatment of MyEnd cells did not lead to activation of the small GTPases Rac1 and RhoA.

weakening of bead binding (76±3%) indicating that TP-mediated improvement of bead binding largely compensated for the loss of anchorage of VE-cadherin to the actin cytoskeleton. We further evaluated effects on the actin cytoskeleton by quantification of F-actin contents in MyEnd cells under the different conditions (Fig. 4C). Cytochalasin D significantly decreased F-actin content (81±6% of controls) whereas TP had no effect (94±4% of controls). These experiments indicated that the action of TP did not involve the actin cytoskeleton.

Alternatively, increased VE-cadherin bead binding could also be explained by activation of intracellular signalling cascades as a result of lateral cross-bridging and clustering of VE-cadherin molecules in response to TP treatment. Members of the Rho family of small GTPases have been shown to be critically involved in regulation of endothelial cell junctions (Vandenbroucke et al., 2008). Therefore, we tested the effect of TP on small GTPases Rac1 and RhoA in GTPase activity assays (Fig. 4D). However, TP treatment did not alter the activity of both small GTPases (95±11% and 111±7% of controls, respectively). Taken together, stabilization of VE-cadherin bead binding by TP was independent of both the actin cytoskeleton and the GTPases Rac1 and RhoA.

TP prevented A23187-mediated reorganization of endothelial adherens junctions

We visualized the effects of A23187 on endothelial adherens junctions in MyEnd cells by VE-cadherin immunostaining. Under control conditions, immunostaining for VE-cadherin showed continuous linear distribution of VE-cadherin along cell junctions (Fig. 5A). Similar results were obtained in the presence of TP for up to 24 hours (not shown). In the presence of A23187, VE-cadherin immunostaining became strongly frayed and fragmented after 45 minutes of incubation (arrows in Fig. 5C). Similar effects have been described for human umbilical vein endothelial cells after treatment with A23187, histamine, vascular endothelial growth factor or TNF-α (Andriopoulou et al., 1999; Esser et al., 1998; Nwariaku et al., 2002; Schnittler et al., 1990). As shown in Fig. 5D-F, TP partially blocked A23187-induced opening and reorganization of adherens junctions. Quantification of frayed and broadened VE-cadherin immunosignals by image thresholding and area measurements confirmed the protective effects of preincubation with TP against A23187-induced changes (Fig. 5G and Materials and Methods for quantification procedure).

Drop of transendothelial electric resistance (TER) in response to mAb 11D4.1 and A23187 was reduced in the presence of TP

Functional changes of endothelial barrier properties were analyzed by TER measurements in endothelial monolayers. First, we used mAb 11D4.1 to evaluate whether VE-cadherin contributes to endothelial barrier properties. Incubation of MyEnd cells with mAb

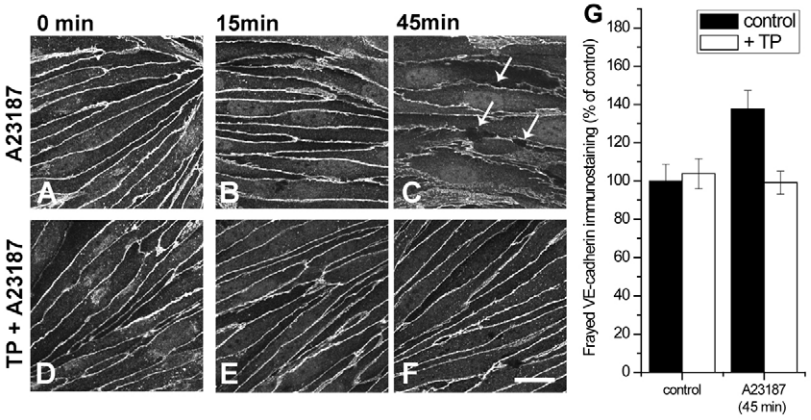

Fig. 5. TP prevented A23187-induced alterations of endothelial adherens junctions. (A-F) Confluent MyEnd monolayers were treated with A23187 (10 μM) for the indicated times. In parallel experiments (D-F), cells were preincubated for 30 minutes with TP (20 μM) before addition of A23187. In controls (0 minutes), VE-cadherin immunostaining was regularly distributed along cell borders (A). Incubation with A23187 led to frayed and fragmented immunostainings after 45 minutes (B,C). This effect was prevented by the presence of TP (D-F). (G) Quantification of VE-cadherin-positive immunosignals confirmed frayed and broadened VE-cadherin staining after 45 minutes incubation with A23187 and the protective effects of preincubation with TP. Images shown are representative of six experiments. Scale bar: 20 μm.

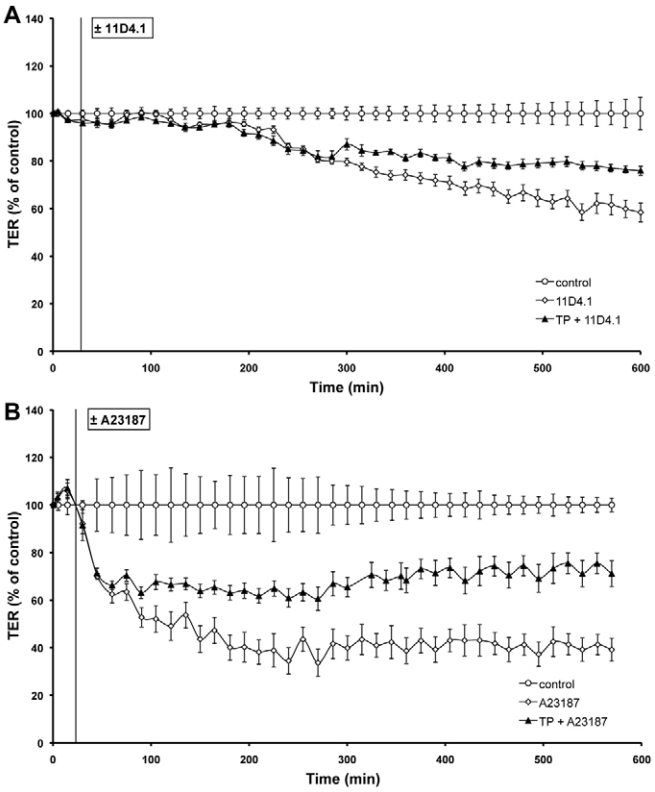

Fig. 6. TP partially prevented loss of TER induced by mAb 11D4.1 and A23187 in endothelial cells. (A) A significant reduction in TER was observed 240 minutes after addition of mAb 11D4.1 (50 µg/ml). Starting after 300 minutes, treatment with TP in addition to mAb 11D4.1 resulted in a significant higher TER compared with mAb 11D4.1 alone (n=5). (B) Treatment of endothelial monolayers with A23187 (10 µM) led to a significant reduction in TER within 45 minutes compared with controls, reaching a plateau after 180 minutes. In endothelial cells preincubated for 30 minutes with 20 µM TP, the A23187-induced drop in TER was partially prevented (n=5).

11D4.1 led to a significant drop of TER (Fig. 6A). After 4 hours, TER was significantly lower in monolayers incubated with mAb 11D4.1 (86±1%) compared with untreated cells (control) and continued to decrease to 58±4% after 10 hours. Pretreatment with TP partially rescued these effects: cells preincubated with TP and treated with mAb 11D4.1 afterwards displayed a similar short-term antibody-induced decrease in TER after 4 hours (86±2%). However, TP prevented a further drop of TER in the following time course (76±2% after 10 hours) when compared to experiments using mAb 11D4.1 alone.

Next, we investigated whether TP would be effective in preventing endothelial barrier breakdown induced by the Ca^{2+} ionophore A23187. In endothelial monolayers treated with 10 µm A23187, TER began to drop after 45 minutes (70±1%) and reached 40±5% of the control resistance after 10 hours (Fig. 6B). Similar to the response shown in Fig. 6A, monolayers pretreated with TP showed an initial drop of TER comparable to cells exposed to A23187 alone (71±2% of control levels after 45 minutes) but no further reduction in TER was observed during the following time course (71±5% after 10 hours). These experiments demonstrated the capability of TP to partially stabilize barrier functions of cultured endothelial monolayers against direct (mAb 11D4.1) or indirect (A23187) stimuli interfering with VE-cadherin-mediated adhesion.

Several other TP concentrations tested ranging from 10 to 200 µM did not improve protective effects assayed by TER measurements (not shown).

TP treatment prevented TNF-α-induced increase of microvessel permeability in vivo

As a final step, we conducted in vivo permeability measurements in single perfused venules of the rat mesentery to test whether TP exerted barrier protective effects in the presence of a clinically relevant mediator of inflammation (Fig. 7). TNF-α was chosen because this cytokine has been shown to play a pivotal role in inflammatory endothelial barrier breakdown partially caused by modulation of VE-cadherin binding (Angelini et al., 2006; Nwariaku et al., 2002; Vandenbroucke et al., 2008). TNF-α alone resulted in significant increase of hydraulic conductivity (L_p) that became obvious after 120 minutes of treatment. A similar lag phase was observed in previous studies (Brett et al., 1989; Goldblum et al., 1993) (Fig. 7A shows representative experiments; Fig. 7B mean L_p values). Simultaneous application of TNF-α and TP, however, completely blocked TNF-α-induced increase of microvascular permeability. After 150 minutes, L_p values in microvessels perfused with TNF-α and TP [2.35±0.55 (cm/second/cm H_2O)×10^{-7}] were not statistically different from controls [1.14±0.33 (cm/second/cm H_2O)×10^{-7}], whereas TNF-α led to strong increase of permeability during this time period [15.13±2.2 (cm/second/cm H_2O)×10^{-7}]. These experiments demonstrated that TP acted as a VE-cadherin-cross-bridging compound stabilizing the endothelial barrier against a physiologically important inflammatory agent.

Discussion

The present study demonstrates that endothelial barrier function can be stabilized by a short dimeric peptide (tandem peptide, TP) derived from the putative binding interface of the N-terminal portion of the outermost VE-cadherin extracellular domain. Our experiments indicate that TP stabilized VE-cadherin transinteraction by its cross-bridging activity. As expected, the monomeric single peptide (SP) sequence blocked homophilic VE-cadherin transinteraction most probably by occupying the site proposed to be involved in binding. TP-induced stabilization of the endothelial barrier was demonstrated in vitro and in vivo by its protective effect against various barrier-compromising stimuli.

Stabilization of VE-cadherin-mediated adhesion is important for maintenance of endothelial barrier function in vitro and in vivo

Our results indirectly indicate that increased intracellular Ca^{2+}, which is known to be a pivotal initial mechanism underlying the effects of most inflammatory mediators (Michel and Curry, 1999; Vandenbroucke et al., 2008), destabilizes the endothelial barrier at least in part via loss of VE-cadherin-mediated binding. This conclusion can be drawn from our observation that TP significantly counteracted A23187-mediated reduction of VE-cadherin binding (laser tweezers) and under these conditions attenuated breakdown of TER.

Since it is difficult to extrapolate from in vitro studies with endothelial monolayers and non-physiological stimuli (mAb 11D4.1, A23187) to the in vivo situation, we tested the barrier stabilizing potency of TP in intact microvessels in vivo using TNF-α as a well established physiological inflammatory stimulus playing a key role in organ dysfunction and death (Cinel and Dellinger, 2007; Opal, 2007). TNF-α disrupts endothelial barrier function via

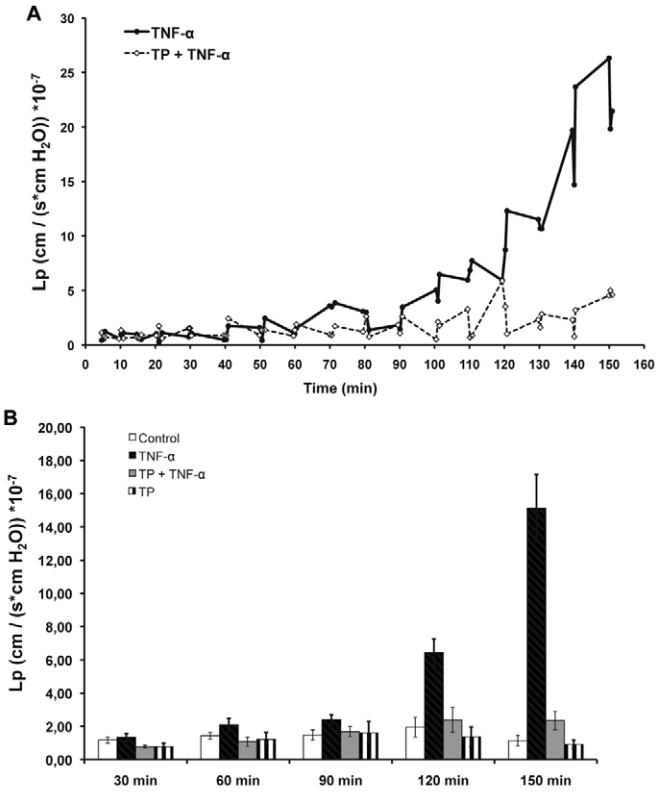

Fig. 7. TP treatment abolished TNF-α-induced increase of microvessel permeability in vivo. (A) Measurements of hydraulic conductivity (L_p) demonstrated that TNF-α strongly increased microvessel permeability, starting after 120 minutes, which was, however, completely prevented by cotreatment with TP. Note that at every time point three independent L_p measurements were made and plotted in this graph. (B) Mean L_p values for each condition show that after 120 minutes TNF-α significantly increased L_p compared with controls. Although having no effect when applied alone, TP completely abolished TNF-α-induced increase of endothelial permeability ($n \geq 5$ for each condition).

several pathways including modulation of VE-cadherin binding (Angelini et al., 2006; Nwariaku et al., 2002). Therefore, we used TNF-α rather than thrombin, which is also known to induce a breakdown of endothelial barrier properties by several pathways in vitro, and is effective in vivo in several vascular beds (Vandenbroucke et al., 2008). However, in microperfused vessels in rat mesentery, thrombin has been reported to have no effect unless venules were previously exposed to inflammatory conditions (Curry et al., 2003). In vivo, simultaneous treatment with TP was effective in blocking TNF-α-induced endothelial hyperpermeability. In view of the crucial role of TNF-α in life-threatening septic inflammation, the present peptide approach to stabilize VE-cadherin transinteraction might be a promising animal model for the treatment of disorders caused by increased vascular leakage.

Tandem peptide mode of action

Single molecule unbinding analysis demonstrated a dose-dependent effect of both TP and SP on VE-cadherin transinteraction. Whereas SP acted as a strong inhibitor of VE-cadherin transinteraction, TP inhibited transinteraction only at high concentrations, at which probably all binding sites of VE-cadherin were occupied by the peptide. Therefore we chose a TP concentration where VE-cadherin transinteraction was not reduced. At lower concentrations (e.g. 20 μM) TP did not inhibit, but rather improved, VE-cadherin transinteraction as indicated by increase of the first peak in unbinding force distributions (see also Baumgartner et al., 2000). Moreover, TP rendered VE-cadherin transinteraction partially resistant against destabilization by an inhibitory antibody. The action of SP and TP was specific for VE-cadherin as concluded from AFM experiments using several control peptides and proteins.

It has to be pointed out that the mode of action of TP probably differs from peptides targeting N-cadherin used by the Doherty group (Williams et al., 2002). In their work, it was demonstrated that agonistic N-cadherin peptides promoted axonal outgrowth via clustering and activation of fibroblast growth factor receptor (FGFR), because inhibition of FGFR prevented agonistic effects of their N-cadherin dimeric peptides. Although a similar mode of action is possible for VE-cadherin TP, our results indicate that cross-bridging of transinteracting VE-cadherin molecules itself is effective to strengthen both VE-cadherin binding and endothelial barrier properties. This can be concluded because TP treatment had protective effects on VE-cadherin transinteraction in cell-free single molecule AFM experiments. Because both lateral clustering and transinteraction of cadherin molecules are known to be a prerequisite for enhanced adhesion (Ahrens et al., 2003; Yap et al., 1997) effects of TP on both interaction mechanisms are likely to contribute to endothelial barrier stabilization in vitro and in vivo. However, interaction of VE-cadherin and vascular endothelial growth factor receptor 2 (VEGFR2) or vascular endothelial protein tyrosine phosphatase has been shown (Carmeliet et al., 1999; Nottebaum et al., 2008), the latter interaction also being targeted by TNF-α. Therefore, we cannot rule out that TP-induced signalling mechanisms in addition to enhanced transinteraction may contribute to the protective effects of TP in vivo and in vitro. However, these effects of TP seem to be independent from small GTPases Rac1 and RhoA as well as from reorganization of the actin cytoskeleton. Furthermore, it has been shown that various inflammatory mediators including VEGF lead to VE-cadherin endocytosis (Gavard and Gutkind, 2006). Blocking cadherin endocytosis by stabilizing cadherin interactions enhanced cellular adhesion as demonstrated for E-cadherin (Troyanovsky et al., 2006). A similar mode of action is also conceivable for TP, further strengthening the hypothesis that TP stabilized VE-cadherin interactions. Nevertheless, short term effects of the VE-cadherin inhibiting agents A23187 or cytochalasin D and protective mechanisms of TP against these agents might not rely on modulation of VE-cadherin endocytosis because we have previously shown that a decrease of surface available VE-cadherin is negligible under these conditions (Baumgartner et al., 2003).

Limitations of the approach to stabilize VE-cadherin binding

A reduced concentration range because of competitive equilibria between displacement reactions at higher concentrations, and between stabilization of lateral clustering and transinteractions, may limit the practical effectiveness of tandem peptide action. This may explain some inconsistencies of TP behaviour in laser tweezer and AFM experiments. Different displacement kinetics could account for TP-mediated enhancement of bead binding: with beads held on the cell surface, there is sufficient time for the displacement and subsequent cross-bridging to occur. With the lifetime of transinteracting VE-cadherin bonds being in the range of $\tau_0 \approx 0.55$ seconds (Baumgartner et al., 2000) and $\tau_0 \approx 2.2$ seconds (Panorchan et al., 2006), displacement and subsequent cross-bridging may not fully develop in AFM experiments. Nevertheless, TP stabilized VE-

cadherin transinteraction in AFM experiments, and dose-dependency curves revealed that no concentration other than 20 μM was more effective at protecting endothelial barrier properties. Apparently, this concentration is also applicable in vivo because TP completely blocked increased microvessel permeability in response to the inflammatory mediator TNF-α.

Finally, even though systemic in vivo application of tandem peptides is most likely to induce severe immune responses, this study is a first step to developing non-peptide drugs that may be useful to protect the endothelial barrier against vascular hyperpermeability.

Materials and Methods

Modelling of the VE-cadherin extracellular domains 1 and 2

A molecular model for the two N-terminal cadherin extracellular domains 1 and 2 (EC1 and 2) of human VE-cadherin was obtained by homology modelling using the crystal structure of E-cadherin [Protein Data Bank (PDB) entry 1EDH] as a template. A multiple sequence alignment was produced using protein sequences of human, mouse and rat VE-cadherin, N-cadherin and E-cadherin with the software CLUSTALW. Amino acid residues differing between VE-cadherin and the structural template were substituted by the corresponding amino acids. Insertions and deletions were modelled manually using the software tool XBUILD in Quanta2006 (Accelrys Inc., San Diego, CA). Close contacts between side chains were first removed by rotamer searches using the XBUILD tool and a subsequent refinement step of the side chain conformer with the lowest starting energy by 100-500 steps of energy minimization using the steepest gradient algorithm and the CHARMm22 force field without electrostatic terms. The resulting final model was further refined by energy minimization and short (50 psecond) molecular dynamics simulations in vacuo with an all-hydrogen force field CHARMM22 without electrostatic terms. In the first rounds, the protein backbone was kept fixed and only side chain atoms were released. Afterwards, the main chain atoms were released stepwise for minimization by employing a positional harmonic potential (initial force constant 50 kcal/mol/Å^2), which was lowered stepwise (at 5 picosecond intervals, the force constant was lowered by 15 kcal/mol/Å^2) to maintain the protein architecture. The final structure model exhibited good backbone and side chain geometries with none of the backbone torsion angles occupying disallowed zones in the Ramachandran plot analysis.

Design of the VE-cadherin single and tandem peptides

The N-terminal N-cadherin domain 1 has been crystallized in three different crystal forms suggesting different assemblies for intermolecular cadherin interactions. The crystal structure from the spacegroup P321 (PDB entry 1NCH) exhibits the largest inter-cadherin interface thus providing the best template for the design of small peptide-based cadherin inhibitors. This assembly is also supported by electron tomography studies on desmosomal knots (He et al., 2003) in which full-length ectodomains are involved in various *trans*- and *cis*-interactions. Another N-cadherin assembly from a N-cadherin EC1-EC2 tandem domain pair suggests a slightly different *trans*-interaction architecture [PDB code 1NCJ (Tamura et al., 1998)], but similar regions as in structure 1NCH are in contact. Other cadherin structures propose differing assemblies in which the N-terminal peptide forms intimate contacts via strand-swapping. Although mutagenesis data for N-cadherin propose a similar interaction with the N-terminal residue Trp2 as the central determinant, we have chosen the assembly from the structure 1NCH because here the interactions are less hydrophobic, possibly yielding peptides with higher solubility. To mimic a putative *cis*-/*trans*-interaction between two VE-cadherin molecules, the crystal structure of the N-terminal cadherin domain 1 was used for docking. The two docked VE-cadherin molecules were refined to remove interfering van der Waals contacts using the CHARMM22 force field without electrostatic term and steepest gradient energy minimization. A single peptide (SP) was designed using residues Arg47 to Glu51 of one VE-cadherin moiety. This peptide segment exhibited tight interaction in terms of intermolecular polar bonds and size of buried surface area. The tandem peptide (TP) was generated by combining two SPs using a flexible linker and cyclization by the addition of cysteine residues.

Test reagents

Single peptide RVDAE and scrambled peptide ADVRE were synthesized in our laboratory using Fmoc-based solid-phase peptide synthesis assembling the peptide on Wang resin. All chemicals were supplied by Novabiochem (Darmstadt, Germany). The tandem peptide sequence was N-Ac-CRVDAE-‘6-aminohexanoic acid linker’-RVDAEC-NH2. The sequences of the control peptides CP1 and CP2 were CLNSMGQDC and CLNSMGQDC-‘6-aminohexanoic acid linker’-CLNSMGQDC, respectively, and derived from a study targeting desmoglein transinteraction with single (CP1) and tandem (CP2) peptides. The underlining of the peptide sequences denotes cyclization via a disulfide bond between the given cysteine residues. TP, CP1 and CP2 peptides were obtained from a commercial supplier (PSL, Heidelberg, Germany). All peptides were purified by reversed-phase HPLC at a purity >95%. After conducting experiments to construct dose-response curves, peptides were used at 200 μM (SP, scrambled, CP1) and 20 μM (TP, CP2), respectively. The monoclonal antibody against the ectodomain of mouse VE-cadherin (11D4.1) has been described previously (Gotsch et al., 1997), was a gift from D. Vestweber (MPI of Molecular Biomedicine, Münster, Germany) and used at 50 μg/ml. A23187 and Cytochalasin D (both from Sigma-Aldrich, Taufkirchen, Germany) were used at 10 μM. Tumor necrosis factor-α (TNF-α; Sigma-Aldrich) was used at 100 ng/ml.

Cell culture

The immortalized murine microvascular endothelial cell line (MyEnd) was grown in Dulbecco’s modified Eagles medium (DMEM, Life Technologies, Karlsruhe, Germany) supplemented with 50 IU/ml penicillin-G, 50 μg streptomycin and 10% fetal calf serum (Biochrom, Berlin, Germany) in a humidified atmosphere (95% air/5% CO_2) at 37°C. VE-cadherin-EYFP-transfected CHO cells (CHO-A1) were cultured as described above with addition of 0.2 g/l geneticin (PAA, Cölbe, Germany). The cultures were used for experiments when grown to confluent monolayers.

Generation of the VE-cadherin-EYFP-expressing cell line CHO-A1

Mouse VE-cadherin full-length cDNA was a kind gift from Dietmar Vestweber (MPI of Molecular Biomedicine), amplified with primers 5′-CCCAAGCTTAT-GCAGAGGCTCACAGAGC-3′ and 5′-GCTCTAGAGATGATGAGTTCCTCC-TGG-3′ and cloned in frame with the cDNA encoding EYFP using *Hin*dIII-*Xba*I-digested plasmid pcDNA3.0-beta2AR-EYFP (a kind gift from Viacheslav Nikolaev, Institute of Pharmacology and Toxicology, University of Würzburg, Germany) to yield pcDNA3.0-VE-cadherin-EYFP. Sequence integrity was confirmed by sequencing. For generation of CHO-A1 cells, the construct was transfected into wild-type Chinese hamster ovary (CHO) cells using Effectene transfection (Qiagen, Hilden, Germany) and a stable-transfected cell line (CHO-A1) was obtained using single cell subsplitting and subsequent characterization for VE-cadherin-EYFP expression.

Atomic force microscopy measurements with recombinant VE-cadherin-Fc

The AFM setup consisted of a Bioscope AFM driven by a Nanoscope III controller (Veeco Instruments, Mannheim, Germany). Homophilic transinteraction of recombinant VE-cadherin was characterized by force-distance measurements of VE-cadherin coupled to Si_3N_4 tips of the cantilever (Veeco Instruments) and freshly cleaved mica plates (SPI Supplies, West Chester, PA) using flexible polyethylene glycol (PEG) spacers containing an amino-reactive crosslinker group at one end and a thiol-reactive group at the other end, as described previously in detail (Baumgartner et al., 2000). If not otherwise stated, binding events were measured in buffer A (140 mM NaCl, 10 mM Hepes, 5 mM $CaCl_2$) by force-distance cycles at amplitudes of 300 nm and 1 Hz frequency yielding continuous trace and retrace velocities of 600 nm/second. For every condition, 300-500 force distance cycles were recorded and each condition was repeated with new cantilever and mica preparations three to four times. Analysis of distribution of single molecule unbinding forces was performed as described previously (Baumgartner et al., 2000). Interaction frequency was evaluated by analyzing and counting specific unbinding events in force distance cycles with a VE-cadherin-coated tip under different conditions thereby reflecting both effective concentrations of VE-cadherin molecules on the tip and binding probabilities. For experiments referring to binding activity, the total area between approach and retrace curves was taken as a measure of adhesion. To investigate VE-cadherin specificity of peptides, SP and TP action on recombinant desmoglein 3-Fc was performed as described recently (Heupel et al., 2008).

Measurements of transendothelial resistance (TER)

ECIS 1600R (Applied BioPhysics, New York, NY) was used to measure the transendothelial resistance (TER) of MyEnd monolayers assessing endothelial barrier integrity as described previously (Baumer et al., 2008) with the following modifications: cells were seeded in wells of the electrode array and grown to confluence for 5-7 days. Before experiments, medium was changed (400 μl DMEM) and in some conditions TP was added. The arrays were plugged into the instrument and preincubated for 30 minutes. A measurement of baseline TER was then performed before the addition of mAb 11D4.1 or A23187.

Cytochemistry

Cells on coverslips were fixed for 10 minutes with 2% formaldehyde in PBS and permeabilized with 0.1% Triton X-100 in PBS for 5 minutes. After rinsing with PBS, cells were preincubated for 30 minutes with 3% normal goat serum/1% bovine serum albumin and incubated for 16 hours at 4°C with rat mAb 11D4.1 (undiluted hybridoma supernatant). After several rinses with PBS (3×5 minutes), monolayers were incubated for 60 minutes at room temperature with Cy3-labelled goat anti-rat IgG (Dianova, Hamburg, Germany) diluted 1:600 in PBS. Coverslips were rinsed with PBS (3×5 minutes) and mounted on glass slides with 60% glycerol in PBS, containing 1.5% *n*-propyl gallate (Serva, Heidelberg, Germany) as anti-fading compound. For quantification of frayed VE-cadherin staining, VE-cadherin-positive signals of six images of each condition (out of three independent experiments) were thresholded, resulting areas were measured and normalized to controls using ImageJ (National Institutes of Health, Bethesda, MD).

Laser tweezer experiments

Coating of polystyrene beads, and laser tweezer experiments were done as described previously (Baumgartner et al., 2003). VE-cadherin-Fc-coated beads were suspended in 250 µl of culture medium and allowed to interact with MyEnd monolayers for 30 minutes at 37°C before initiation of experiments. For some experiments, TP had been preincubated on cells prior to bead incubation or agents (A23187, cytochalasin D or mAb 11D4.1) have been applied to surface-bound beads. Beads were considered tightly bound when resisting laser displacement at 42 mW setting of the home-built laser tweezer setup consisting of a Nd:YAG laser (1064 nm, Laser 2000, Wessling, Germany) and Axiovert 135 microscope (Zeiss, Oberkochen, Germany) equipped with a high NA objective (63× 1.2 oil, Zeiss) and a piezo-driven XY position table. For every condition 100 beads were counted and every condition repeated six times. The percentage of beads resisting laser displacement under various experimental conditions was normalized to control values.

Quantification of F-actin

Quantification of F-actin was performed as described previously (Waschke et al., 2004). In brief, MyEnd cells were fixed with formaldehyde and permeabilized with Triton X-100. Then, phalloidin covalently labelled with Alexa Fluor 488 (Mobitec, Goettingen, Germany; 1:60) was incubated on cells for 1 hour at 37°C. After washing, phalloidin-Alexa Fluor 488 was extracted from cells by two subsequent 1-hour incubation steps with 1 ml of methanol at 37°C. Methanol supernatants were centrifuged at 100,000 × ***g*** for 20 minutes and quantified with a FITC filter on a Victor plate reader (PerkinElmer, Waltham, MA, USA).

Rac1 and RhoA activation assay

For measurement of Rac1 or RhoA activation in MyEnd cells upon TP treatment, Rac1 or RhoA G-Lisa activation assays (Cytoskeleton, Denver CO, USA) using Rac1-GTP or RhoA-GTP binding domain-coated plates, respectively, were used according to the manufacturer's recommendations (Baumer et al., 2008).

Fluorescence recovery after photobleaching (FRAP) studies

CHO-A1 cells were transferred to live cell imaging chambers, covered with phenol red-free DMEM medium (Sigma-Aldrich) and placed on a 37°C-heated objective. Then, regions of interest at sites of cell-cell contacts were selected and bleaching series were performed using the 514 nm line of an argon laser coupled to a confocal laser scanning microscope (CLSM 5, Zeiss). Region of interest fluorescence intensity measurements of recorded images were analyzed using ImageJ (National Institutes of Health). All values were corrected for background fluorescence and loss in fluorescence due to scanning frequency. For comparison between different conditions, fluorescence intensity values were normalized to pre-bleach values and first post-bleach values set to zero.

In vivo measurements of hydraulic conductivity (L_p)

Preparation and anaesthetizing of Wistar rats were performed as described previously (Waschke et al., 2004). Rats were kept under conditions that conformed to the National Institutes of Health 'Guide for the Care and Use of Laboratory Animals', approved by the Regierung of Unterfranken. All experiments were carried out in straight non-branched segments of venular microvessels (25-35 µm in diameter) in mesentery of living rats. Measurements were based on the modified Landis technique, which measures the volume flux (J_v/S) per unit surface area across the wall of a microvessel perfused via a glass micropipette following single occlusion of the vessel at usually 50 cm H_2O (Michel and Curry, 1999). All perfusates were mammalian Ringer solutions containing serum albumin at 10 mg/ml (Sigma-Aldrich). Hydraulic conductivity (L_p; or hydraulic permeability) was estimated for each occlusion as $(J_v/S)/P_{eff}$ and measurements were made at approximately 10-minute intervals for up to 160 minutes. In some conditions, TNF-α and/or TP were added to the perfusate and continuously delivered via the micropipette. In preliminary dose-response experiments, TNF-α was found to consistently increase permeability of mesenteric postcapillary venules at a concentration of 100 ng/ml. For every condition, at least five vessels from different rats were used.

Statistics

Values throughout are expressed as mean ± s.e.m. Nonparametric Mann-Whitney tests were used to test for differences in L_p groups because baseline L_p distributions are non-Gaussian in rat mesentery venules (Huxley and Rumbaut, 2000; Michel et al., 1974). Otherwise, possible differences were assessed using unpaired Student's *t*-test. Statistical significance was assumed for $P<0.05$.

We dedicate this paper to the late Rainer Koob, who synthesized the first peptides and provided critical input into this study. We thank Christian Rankl and Peter Hinterdorfer (University of Linz, Austria) for providing AFM analysis software and help with its use, Hermann Gruber (University of Linz, Austria) for providing the AFM PEG linker and Albert Sickmann (Rudolf Virchow Center, Würzburg, Germany) for analyzing peptides by mass spectrometry. We are grateful to Lisa Bergauer, Tanja Franzeskakis, Nadja Niedermeier, Tanja Reimer and Alexia Witchen for skilful technical assistance. These studies were supported in part by grants from the Deutsche Forschungsgemeinschaft (SFB 487, TP B2 and B5 and SFB 688, TP A4).

References

Ahrens, T., Lambert, M., Pertz, O., Sasaki, T., Schulthess, T., Mege, R. M., Timpl, R. and Engel, J. (2003). Homoassociation of VE-cadherin follows a mechanism common to "classical" cadherins. *J. Mol. Biol.* **325**, 733-742.

Alexander, J. S. and Elrod, J. W. (2002). Extracellular matrix, junctional integrity and matrix metalloproteinase interactions in endothelial permeability regulation. *J. Anat.* **200**, 561-574.

Andriopoulou, P., Navarro, P., Zanetti, A., Lampugnani, M. G. and Dejana, E. (1999). Histamine induces tyrosine phosphorylation of endothelial cell-to-cell adherens junctions. *Arterioscler. Thromb. Vasc. Biol.* **19**, 2286-2297.

Angelini, D. J., Hyun, S. W., Grigoryev, D. N., Garg, P., Gong, P., Singh, I. S., Passaniti, A., Hasday, J. D. and Goldblum, S. E. (2006). TNF-alpha increases tyrosine phosphorylation of vascular endothelial cadherin and opens the paracellular pathway through fyn activation in human lung endothelia. *Am. J. Physiol. Lung Cell Mol. Physiol.* **291**, L1232-L1245.

Angst, B. D., Marcozzi, C. and Magee, A. I. (2001). The cadherin superfamily. *J. Cell Sci.* **114**, 625-626.

Baumer, Y., Drenckhahn, D. and Waschke, J. (2008). cAMP induced Rac 1-mediated cytoskeletal reorganization in microvascular endothelium. *Histochem. Cell Biol.* **129**, 765-778.

Baumgartner, W., Hinterdorfer, P., Ness, W., Raab, A., Vestweber, D., Schindler, H. and Drenckhahn, D. (2000). Cadherin interaction probed by atomic force microscopy. *Proc. Natl. Acad. Sci. USA* **97**, 4005-4010.

Baumgartner, W., Schutz, G. J., Wiegand, J., Golenhofen, N. and Drenckhahn, D. (2003). Cadherin function probed by laser tweezer and single molecule fluorescence in vascular endothelial cells. *J. Cell Sci.* **116**, 1001-1011.

Boggon, T. J., Murray, J., Chappuis-Flament, S., Wong, E., Gumbiner, B. M. and Shapiro, L. (2002). C-cadherin ectodomain structure and implications for cell adhesion mechanisms. *Science* **296**, 1308-1313.

Brett, J., Gerlach, H., Nawroth, P., Steinberg, S., Godman, G. and Stern, D. (1989). Tumor necrosis factor/cachectin increases permeability of endothelial cell monolayers by a mechanism involving regulatory G proteins. *J. Exp. Med.* **169**, 1977-1991.

Carmeliet, P., Lampugnani, M. G., Moons, L., Breviario, F., Compernolle, V., Bono, F., Balconi, G., Spagnuolo, R., Oostuyse, B., Dewerchin, M. et al. (1999). Targeted deficiency or cytosolic truncation of the VE-cadherin gene in mice impairs VEGF-mediated endothelial survival and angiogenesis. *Cell* **98**, 147-157.

Cinel, I. and Dellinger, R. P. (2007). Advances in pathogenesis and management of sepsis. *Curr. Opin. Infect. Dis.* **20**, 345-352.

Corada, M., Mariotti, M., Thurston, G., Smith, K., Kunkel, R., Brockhaus, M., Lampugnani, M. G., Martin-Padura, I., Stoppacciaro, A., Ruco, L. et al. (1999). Vascular endothelial-cadherin is an important determinant of microvascular integrity *in vivo*. *Proc. Natl. Acad. Sci. USA* **96**, 9815-9820.

Curry, F. E., Joyner, W. L. and Rutledge, J. C. (1990). Graded modulation of frog microvessel permeability to albumin using ionophore A23187. *Am. J. Physiol.* **258**, H587-H598.

Curry, F. E., Zeng, M. and Adamson, R. H. (2003). Thrombin increases permeability only in venules exposed to inflammatory conditions. *Am. J. Physiol. Heart Circ. Physiol.* **285**, H2446-H2453.

Dejana, E., Orsenigo, F. and Lampugnani, M. G. (2008). The role of adherens junctions and VE-cadherin in the control of vascular permeability. *J. Cell Sci.* **121**, 2115-2122.

Esser, S., Lampugnani, M. G., Corada, M., Dejana, E. and Risau, W. (1998). Vascular endothelial growth factor induces VE-cadherin tyrosine phosphorylation in endothelial cells. *J. Cell Sci.* **111**, 1853-1865.

Gavard, J. and Gutkind, J. S. (2006). VEGF controls endothelial-cell permeability by promoting the beta-arrestin-dependent endocytosis of VE-cadherin. *Nat. Cell Biol.* **8**, 1223-1234.

Goldblum, S. E., Ding, X. and Campbell-Washington, J. (1993). TNF-alpha induces endothelial cell F-actin depolymerization, new actin synthesis, and barrier dysfunction. *Am. J. Physiol.* **264**, C894-C905.

Gotsch, U., Borges, E., Bosse, R., Boggemeyer, E., Simon, M., Mossmann, H. and Vestweber, D. (1997). VE-cadherin antibody accelerates neutrophil recruitment *in vivo*. *J. Cell Sci.* **110**, 583-588.

Gumbiner, B. M. (2000). Regulation of cadherin adhesive activity. *J. Cell Biol.* **148**, 399-404.

He, P. and Curry, F. E. (1991). Depolarization modulates endothelial cell calcium influx and microvessel permeability. *Am. J. Physiol.* **261**, H1246-H1254.

He, W., Cowin, P. and Stokes, D. L. (2003). Untangling desmosomal knots with electron tomography. *Science* **302**, 109-113.

Heupel, W. M., Zillikens, D., Drenckhahn, D. and Waschke, J. (2008). Pemphigus vulgaris IgG directly inhibit desmoglein 3-mediated transinteraction. *J. Immunol.* **181**, 1825-1834.

Heupel, W. M., Muller, T., Efthymiadis, A., Schmidt, E., Drenckhahn, D. and Waschke, J. (2009). Peptides targeting the desmoglein 3 adhesive interface prevent autoantibody-induced acantholysis in pemphigus. *J. Biol. Chem.* **284**, 8589-8595.

Hordijk, P. L., Anthony, E., Mul, F. P., Rientsma, R., Oomen, L. C. and Roos, D. (1999). Vascular-endothelial-cadherin modulates endothelial monolayer permeability. *J. Cell Sci.* **112**, 1915-1923.

Huxley, V. H. and Rumbaut, R. E. (2000). The microvasculature as a dynamic regulator of volume and solute exchange. *Clin. Exp. Pharmacol. Physiol.* **27**, 847-854.
Konstantoulaki, M., Kouklis, P. and Malik, A. B. (2003). Protein kinase C modifications of VE-cadherin, p120, and beta-catenin contribute to endothelial barrier dysregulation induced by thrombin. *Am. J. Physiol. Lung Cell Mol. Physiol.* **285**, L434-L442.
Michel, C. C. and Curry, F. E. (1999). Microvascular permeability. *Physiol. Rev.* **79**, 703-761.
Michel, C. C., Mason, J. C., Curry, F. E., Tooke, J. E. and Hunter, P. J. (1974). A development of the Landis technique for measuring the filtration coefficient of individual capillaries in the frog mesentery. *Q. J. Exp. Physiol. Cogn. Med. Sci.* **59**, 283-309.
Nagar, B., Overduin, M., Ikura, M. and Rini, J. M. (1996). Structural basis of calcium-induced E-cadherin rigidification and dimerization. *Nature* **380**, 360-364.
Navarro, P., Caveda, L., Breviario, F., Mandoteanu, I., Lampugnani, M. G. and Dejana, E. (1995). Catenin-dependent and -independent functions of vascular endothelial cadherin. *J. Biol. Chem.* **270**, 30965-30972.
Nottebaum, A. F., Cagna, G., Winderlich, M., Gamp, A. C., Linnepe, R., Polaschegg, C., Filippova, K., Lyck, R., Engelhardt, B., Kamenyeva, O. et al. (2008). VE-PTP maintains the endothelial barrier via plakoglobin and becomes dissociated from VE-cadherin by leukocytes and by VEGF. *J. Exp. Med*. **205**, 2929-2945.
Nwariaku, F. E., Liu, Z., Zhu, X., Turnage, R. H., Sarosi, G. A. and Terada, L. S. (2002). Tyrosine phosphorylation of vascular endothelial cadherin and the regulation of microvascular permeability. *Surgery* **132**, 180-185.
Opal, S. M. (2007). The host response to endotoxin, antilipopolysaccharide strategies, and the management of severe sepsis. *Int. J. Med. Microbiol.* **297**, 365-377.
Panorchan, P., George, J. P. and Wirtz, D. (2006). Probing intercellular interactions between vascular endothelial cadherin pairs at single-molecule resolution and in living cells. *J. Mol. Biol.* **358**, 665-674.
Rabiet, M. J., Plantier, J. L. and Dejana, E. (1994). Thrombin-induced endothelial cell dysfunction. *Br. Med. Bull.* **50**, 936-945.
Rabiet, M. J., Plantier, J. L., Rival, Y., Genoux, Y., Lampugnani, M. G. and Dejana, E. (1996). Thrombin-induced increase in endothelial permeability is associated with changes in cell-to-cell junction organization. *Arterioscler. Thromb. Vasc. Biol.* **16**, 488-496.
Schnittler, H. J., Wilke, A., Gress, T., Suttorp, N. and Drenckhahn, D. (1990). Role of actin and myosin in the control of paracellular permeability in pig, rat and human vascular endothelium. *J. Physiol.* **431**, 379-401.
Shapiro, L., Fannon, A. M., Kwong, P. D., Thompson, A., Lehmann, M. S., Grubel, G., Legrand, J. F., Als-Nielsen, J., Colman, D. R. and Hendrickson, W. A. (1995). Structural basis of cell-cell adhesion by cadherins. *Nature* **374**, 327-337.
Stehbens, S. J., Paterson, A. D., Crampton, M. S., Shewan, A. M., Ferguson, C., Akhmanova, A., Parton, R. G. and Yap, A. S. (2006). Dynamic microtubules regulate the local concentration of E-cadherin at cell-cell contacts. *J. Cell Sci.* **119**, 1801-1811.
Steinberg, M. S. and McNutt, P. M. (1999). Cadherins and their connections: adhesion junctions have broader functions. *Curr. Opin. Cell Biol.* **11**, 554-560.
Tamura, K., Shan, W. S., Hendrickson, W. A., Colman, D. R. and Shapiro, L. (1998). Structure-function analysis of cell adhesion by neural (N-) cadherin. *Neuron* **20**, 1153-1163.
Troyanovsky, R. B., Sokolov, E. P. and Troyanovsky, S. M. (2006). Endocytosis of cadherin from intracellular junctions is the driving force for cadherin adhesive dimer disassembly. *Mol. Biol. Cell* **17**, 3484-3493.
Vandenbroucke, E., Mehta, D., Minshall, R. and Malik, A. B. (2008). Regulation of endothelial junctional permeability. *Ann. NY Acad. Sci.* **1123**, 134-145.
Waschke, J., Baumgartner, W., Adamson, R. H., Zeng, M., Aktories, K., Barth, H., Wilde, C., Curry, F. E. and Drenckhahn, D. (2004). Requirement of Rac activity for maintenance of capillary endothelial barrier properties. *Am. J. Physiol. Heart Circ. Physiol.* **286**, H394-H401.
Williams, G., Williams, E. J. and Doherty, P. (2002). Dimeric versions of two short N-cadherin binding motifs (HAVDI and INPISG) function as N-cadherin agonists. *J. Biol. Chem.* **277**, 4361-4367.
Yap, A. S., Brieher, W. M., Pruschy, M. and Gumbiner, B. M. (1997). Lateral clustering of the adhesive ectodomain: a fundamental determinant of cadherin function. *Curr. Biol.* **7**, 308-315.

Journal of Cell Science